ELSEVIER

Journal of Photochemistry and Photobiology A: Chemistry 141 (2001) 209–217

Journal of Photochemistry and Photobiology A:Chemistry

www.elsevier.nl/locate/jphotochem

Photocatalytic activity of WO_x-TiO_2 under visible light irradiation

X.Z. Li [a,*], F.B. Li [a], C.L. Yang [b], W.K. Ge [b]

[a] *Department of Civil and Structural Engineering, The Hong Kong Polytechnic University, Hunghom, Kowloon, Hong Kong, PR China*
[b] *Department of Physics, Hong Kong University of Science and Technology, Clear Water Bay, Kowloon, Hong Kong, PR China*

Received 17 January 2001; received in revised form 21 March 2001; accepted 4 April 2001

Abstract

With an attempt to extend light absorption of the TiO_2-based photocatalysts toward the visible light range and eliminate the rapid recombination of excited electrons/holes during photoreaction, new photocatalyst (WO_x-TiO_2) powder was prepared by a sol–gel method. The photooxidation efficiency of WO_x-TiO_2 catalyst was also evaluated by conducting a set of experiments to photodegrade methylene blue (MB) in aqueous solution. The photocatalytic activity of WO_x-TiO_2 was examined by X-ray diffraction (XRD), UV–VIS absorption spectra, X-ray photoelectron emission spectroscopy (XPS), photoluminescence spectra (PL), surface photovoltage spectra (SPS) and electron-field-induced surface photovoltage spectra (EFISPS). The experiments demonstrated that the MB in aqueous solution was successfully photodegraded using WO_x-TiO_2 under visible light irradiation. It was found that an optimal WO_x dosage of 3% in WO_x-TiO_2 achieved the highest rate of MB photodegradation in this experimental condition. It has been confirmed that WO_x-TiO_2 could be excited by visible light ($E < 3.2$ eV) and the recombination rate of electrons/holes in WO_x-TiO_2 declined due to the existence of WO_3 doped in TiO_2. The order of its photoactivity from weak to strong had a good agreement with that of PL intensity and that of EFISPS intensity from strong to weak.

Keywords: Photocatalytic properties; Titanium dioxide; Tungsten oxide; Photoluminescence spectra; Surface photovoltage spectra; Methylene blue

1. Introduction

The degradation of organic pollutants in water by photocatalysis, using the wide optical band gap material (TiO_2), has attracted extensive attention during recent 20 years [1]. Many researchers have proved that semiconductor, TiO_2, is an excellent photocatalyst, which can break down most kinds of refractory organic pollutants, including detergents, dyes, pesticides and herbicides under UV-light irradiation [2,3]. However, it has been also known that this type of photooxidation has two typical defects: firstly TiO_2 is a high energy band ($E_g \approx 3.2$ eV) material that can only be excited by high energy UV irradiation with a wavelength of no longer than 387.5 nm. This practically rules out the use of sunlight as an energy source for the photoreaction. Secondly, a low rate of electron transfer to oxygen and a high rate of recombination between excited electron/hole pairs result in a low quantum yield rate and also a limited photooxidation rate [4–6]. Recently, there are a number of studies related to the photocatalytic activity of metal oxide-TiO_2 catalysts for the purpose of improving TiO_2 photocatalytic activity, including CdS [5,6], SnO_2 [7,8], WO_3 [9–12], SiO_2 [13,14], ZrO_2 [15], V_2O_5 [16]. Coupled semiconductor photocatalysts may increase the efficiency of photocatalytic process by increasing the charge separation and extending the energy range of photoexcitation. At the same time, its physical and optical properties are greatly modified. Up to now, several studies focused on the optical properties of metal ion-doped TiO_2 [17–19]. The Pb impurity makes it possible for TiO_2 to absorb visible light. The impurity energy level such as V, Cr, Mn and Fe doped in single crystalline rutile TiO_2 was investigated by photocurrent measurement and theoretical calculations, and the broad absorption band in visible range was ascribable to metal ion doping [20–22]. The use of selective catalytic reduction (SCR) based on vanadium-tungsten oxide-TiO_2 catalysts has been mostly related to air pollution control [9,11,12,23–26]. Do et al. [10] found the degradation rate of 1,4-dichlorobenzene was enhanced by addition of WO_3 on the surface of TiO_2. However, WO_x-TiO_2 mentioned above was prepared by physical mixing [9], multi-step grafting of ammonium tungstate [10–12], and WO_x only wrapped on the surface of TiO_2.

In this study, WO_x-TiO_2 samples were prepared by a sol–gel process with the aims of (i) extending the light absorption spectrum toward the visible region; (ii) hindering

* Corresponding author. Tel.: +852-2766-6016; fax: +852-2334-6389.
E-mail address: cexzli@polyu.edu.hk (X.Z. Li).

1010-6030/01/$ – see front matter
PII: S1010-6030(01)00446-4

the recombination of electron/hole pairs; and (iii) disclosing the relationship between photocatalytic properties and photoactivity.

2. Experimental

2.1. Preparation of WOx-TiO_2 catalysts

The WO_x-TiO_2 samples with different WO_x fraction were synthesized by the sol–gel process. A 0.05 mol TiO_2 transparent sol was first prepared using Ti(O-Bu)$_4$, 120 ml absolute ethanol, 15 ml acetic acid, and 5 ml doubly distilled water, and aged for 1 day. Then 3.0 ml aqueous solution of ammonium tungstate $(NH_4)_{10}H_2W_{12}O_{42}\cdot 4H_2O$ was added drop-wise to the sol under vigorous stirring for 2 h until WO_x-TiO_2 gel formed. WO_x-TiO_2 sample was obtained in a doping level of 1.5% after aged, dried, ground and sintered at 973 K for 2 h, and labeled as 1.5%WO_x-TiO_2. Similarly, 3, 4, 5, and 10%WO_x-TiO_2 samples were also prepared according to the above procedure. All doping concentration mentioned in this work was the nominal molar concentration, which was based upon the assumption of quantitative fraction of WO_3. All chemicals used in this work were of analytical grade, and doubly distilled water was used for the solution preparation.

2.2. Characterization of photocatalysts

To determine the crystal phase composition of the prepared photocatalysts (WO_x-TiO_2), X-ray diffraction (XRD) measurement was carried out at room temperature using a Rigaku D/MAX-IIIA diffractometer with Cu Kα radiation ($\lambda = 0.15418$ nm). The accelerating voltage of 35 kV and emission current of 30 mA were used. To determine the light absorption band after the WO_x doping in the structure of TiO_2, a thin film of WO_x-TiO_2 was prepared and its UV–VIS absorption spectra of the photocatalysts were measured in the range of 250–700 nm using a UV–VIS Scanning Spectrophotometer (Shimadzu UV-2101 PC). To study the recombination of electrons/holes in the photocatalysts, the photoluminescence (PL) emission spectra of the samples were measured in the following procedure: firstly, at room temperature, a 325 nm He–Cd laser was used as an excitation light source; then, the light from the sample was focused into a spectrometer (Spex500) and detected by a photo multiplier tube (PMT); and finally, the signal from the PMT was input into a photon counter (SR400) before recorded by a computer. To study the valance state of the photocatalysts, X-ray photoelectron spectroscopy (XPS) was recorded with the PHI Quantum ESCA Microprobe System, using the Mg Kα line of a 250 W Mg X-ray tube as a radiation source with the energy of 1253.6 eV, 16 mA × 12.5 kV and a working pressure lower than 1×10^{-8} N m^{-2}. As an internal reference for the absolute binding energies, the C1s peak of hydrocarbon contamination was used. The fitting of XPS curves was analyzed with a software (Multipak 6.0 A). To study the photovoltage response and energy level, surface photovoltage spectra (SPS) and electron-field induced surface photovoltage spectra (EFISPS) were obtained using a photovoltaic cell by a light source-monochromator-lock-in detection technique. Monochromatic light was obtained by passing light from a 500 W xenon lamp through a double prism monochromator. A lock-in amplifier, synchronized with a light chopper was used to amplify the photovoltage signal. The photovoltages were normalized so that the intensities of monochromatic light incident on the surface of the samples were constant.

2.3. Equipment and experimental procedure

A cylindrical Pyrex photoreactor was used in the study as shown in Fig. 1, in which a 110 W high-pressure sodium lamp (Institute of Electrical Light Source, Beijing) was positioned inside the cylindrical Pyrex vessel surrounded by a circulating water jacket (Pyrex) to cool the reaction solution. The photoemission spectrum of the high pressure sodium lamp is illustrated in Fig. 2, which mainly provides visible light in the range of 400–800 nm.

Reaction suspensions were prepared by adding 0.2 g WO_x-TiO_2 powder into a 165 ml of aqueous methylene blue (MB) solution with an initial concentration of 12.5 mg l^{-1}. The analytical grade MB chemical was provided by BDH and used without further purification. Prior to photooxidation, the suspension was magnetically stirred in a dark condition for 15 min to establish an adsorption/desorption equilibrium condition. The aqueous suspension containing MB and photocatalyst were irradiated under the visible

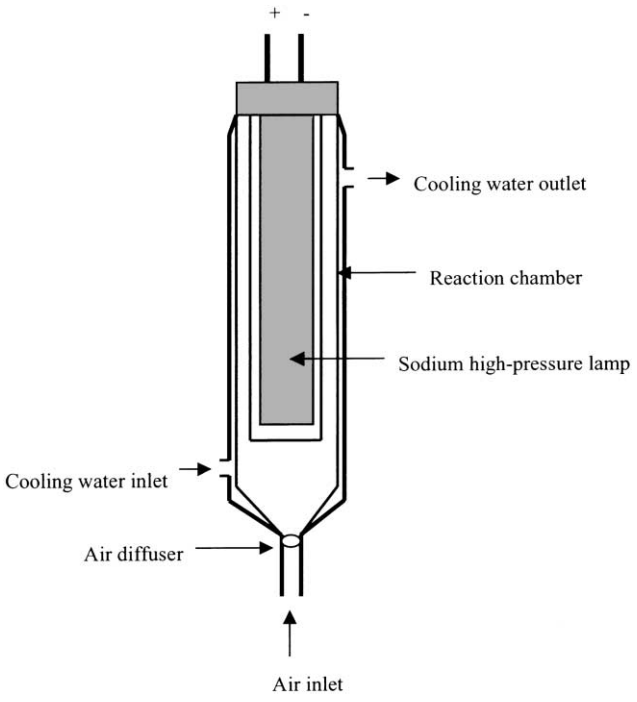

Fig. 1. A sketch of photoreactor.

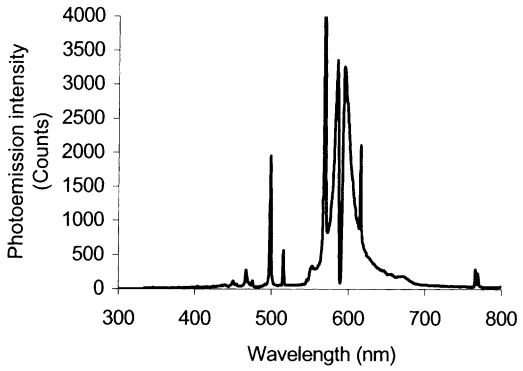

Fig. 2. The photoemission spectra of the high-pressure sodium lamp.

light with constant aeration. At the given time intervals, analytical samples were taken from the suspension and immediately centrifuged at 70 rps for 20 min, then filtered through a 0.45 μm Millipore filter to remove the particles. The filtrate was then analyzed as required.

2.4. Analytical methods

MB concentration was analyzed by a UV–VIS spectroscopy (Spectronic Genesys-2) at 664 nm. TOC concentration was determined by a TOC-analyzer (Shimadzu 5000A) equipped with an auto-sampler (ASI-5000).

3. Results and discussion

3.1. Photocatalytic oxidation

The efficiency of photocatalytic oxidation using the WO_x-TiO_2 samples was evaluated on the basis of the photodegradation rate of MB in aqueous solution. The experimental data demonstrated that MB photodegradation followed the pseudo-first-order kinetics with respect to MB concentration. The observed rate constants of MB photodegradation using pure TiO_2 and the TiO_2 doped with 1.5, 3, 4, 5, and 10% WO_x are illustrated in Fig. 3, respectively. It was found that the observed photooxidation rate using the pure TiO_2 was much lower than that using WO_x-TiO_2. The reaction of MB photodegradation showed that the WO_x impurity doped in TiO_2 could enhance the photocatalytic activity of TiO_2 significantly. While the impurity fraction of WO_x in TiO_2 increased, the rate of MB photodegradation increased initially and then decreased when the WO_x content exceeds 3%. This implies there was an optimum molar content of $WO_x = 3\%$.

The removal of TOC was also studied in order to disclose the mineralization degree of MB solution and the experimental results are shown in Fig. 4. Six samples were collected at the time intervals of 0, 20, 40, 60, 80, 100 min. After the irradiation of 100 min, the removal percent of TOC was achieved

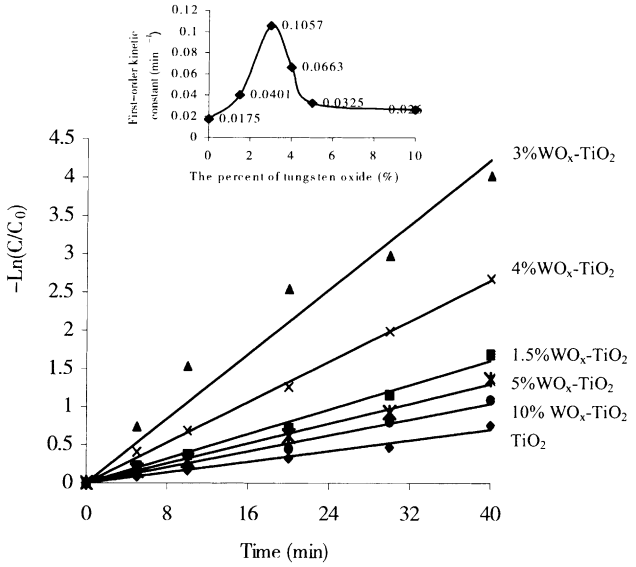

Fig. 3. The photocatalytic degradation of MB in WO_x-TiO_2 suspensions with $C_0 = 12.5\,mg\,l^{-1}$ irradiated by the 110 W high-pressure sodium lamp at pH 5.86.

to 41.2, 83.5 and 60.4% using pure TiO_2, 3%WO_x-TiO_2 and 5%WO_x-TiO_2, respectively. The 3%WO_x-TiO_2 was the most photoactive to degrade MB in this experimental condition.

3.2. Iso-electric point and specific area

To understand the adsorption behavior of the modified TiO_2 catalyst in its aqueous solution, the zeta (ς) potentials of TiO_2 and 3%WO_x-TiO_2 samples were measured in the pH range of 2.0–8.5, and the iso-electric points of samples were determined as pH 6.40 and 5.00, respectively, as shown in Fig. 5. The results demonstrated that the iso-electric point of modified TiO_2 catalyst was reduced from pH 6.4 to around 5. It is believed that the iso-electric point would greatly influence the adsorption of organic substrates and its intermediates on the surface of photocatalyst during photoreaction. In fact, the photocatalytic process mainly occurs on the photocatalyst surface, but not in bulk solution. The

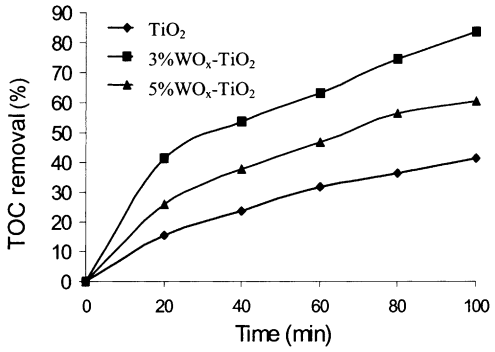

Fig. 4. The TOC removal during MB photodegradation.

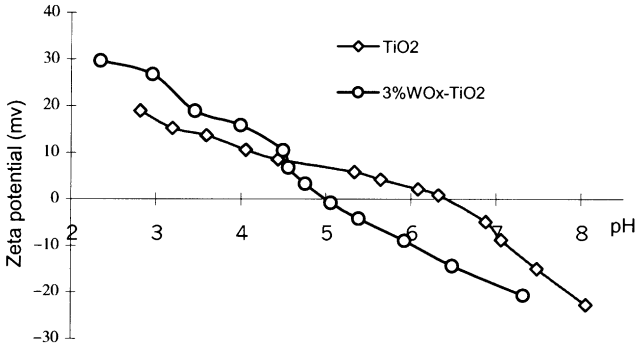

Fig. 5. Iso-electric points of pure TiO_2 and 3%WO_x-TiO_2.

Table 1
Particle size and specific area of photocatalysts

Samples	Particle size (nm)	Specific area ($m^2\,g^{-1}$)
TiO_2	29.5	73.2
3%WO_x/TiO_2	23.4	85.1
5%WO_x/TiO_2	22.5	114.8

adsorption of substrates is indispensable for their photocatalytic degradation. As a cationic dye, MB was more easily adsorbed on the 3%WO_x-TiO_2 surface than the pure TiO_2. This is one of reasons why the photoactivity of tungsten oxide modified TiO_2 was higher than that of pure TiO_2. Moreover, the increased specific area and finer particle size of the 3%WO_x-TiO_2 as shown in Table 1 may be another reason to enhance the photocatalytic behavior of tungsten oxide modified TiO_2 as previously reported by the authors [27].

3.3. XRD analysis

It has been reported by several studies [3,9,11] that sol–gel sample of TiO_2 should undergo a phase transformation from anatase to rutile during sintering treatment. The higher sintering temperature would form more rultile phase in general. In this study, all the samples were sintered at 973 K and their diffractograms are described in Fig. 6. The spectrum results indicated that all the WO_x-TiO_2 samples contained lower fraction of rutile than the pure TiO_2, which means the phase transmission was less significant during the sintering of the WO_x-TiO_2 samples at 973 K. For the pure TiO_2, the results showed that it had undergone a major phase transformation from anatase to rutile, and only a small anatase peak of 101 plane present. However, for all the WO_x-TiO_2 samples, the main phase was still anatase phase, and only rutile peak of 002 plane present. Obviously, tungsten oxides hindered the phase transformation from anatase to rutile during sintering. With the increase of tungsten oxides, new peaks appeared at $2\theta = 20.45$ and 22.83° for the 5%WO_x-TiO_2. The new peaks may be attributable to a new component of $W_xTi_{1-x}O_2$.

3.4. XPS analysis

The XPS analysis was carried out to determine the chemical composition of the catalysts and the valence states of various species present therein. The Ti 2p XPS spectra of all samples are shown in Fig. 7A. For the pure TiO_2, the Ti 2p peaks are narrow with slight asymmetry and have a binding energy of 458.63 eV (FWHM = 1.14 eV), attributed to Ti^{4+}. For the 3%WO_x-TiO_2, the spectrum appears in a wide range (FWHM = 1.67 eV) and its intensity decreased, perhaps due to tungsten oxides being doped in the lattice of TiO_2. The binding energy was 0.36 eV, less than that of TiO_2. There was no any fitting peak of Ti^{3+} for the 3%WO_x-TiO_2. However, Xiao et al. [28] reported Ar ion bombardment induced the change of Ti chemical state of TiO_2 and the concentration of Ti^{3+} increased. Similarly in this study, the O 1s XPS spectra show a two-band structure for the 3%WO_x-TiO_2 as described in Fig. 7B and Table 2. A dominant peak at

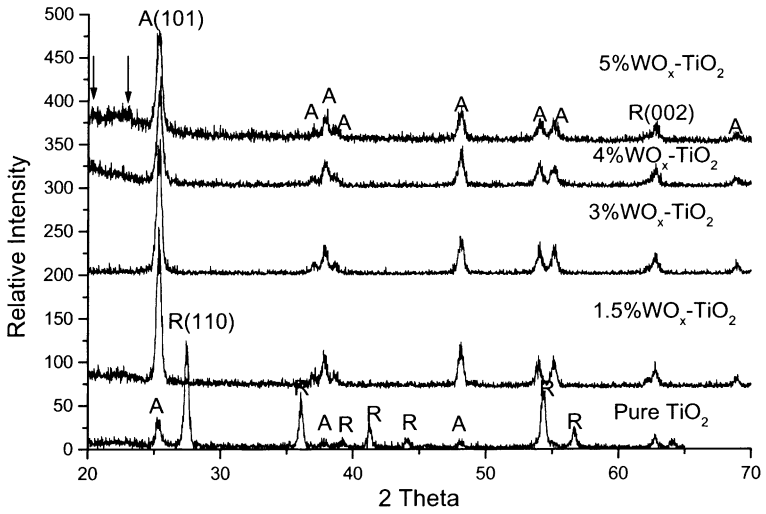

Fig. 6. The XRD photograph of WO_x-TiO_2.

Table 2
O 1s, Ti 2p, W 4f XPS data and their valence states obtained from the fitted curve

Catalysts	TiO_2			3%WO_x-TiO_2		
	Binding energy (eV)	FWHM[a] (eV)	Area (%)	Binding energy (eV)	FWHM[a] (eV)	Area (%)
O 1s 1/2	529.93	1.27	100	529.85	1.64	35.94
O 1s 2/2				530.58	1.36	63.06
Ti 2p (IV)	458.63	1.14	100	458.27	1.67	100.00
WO_3				37.88	1.70	60.70
W_xO_y				36.14	1.70	36.91
WO_2				33.29	1.25	2.39

[a] FWHM: full width at one-half of the maximum height of peaks.

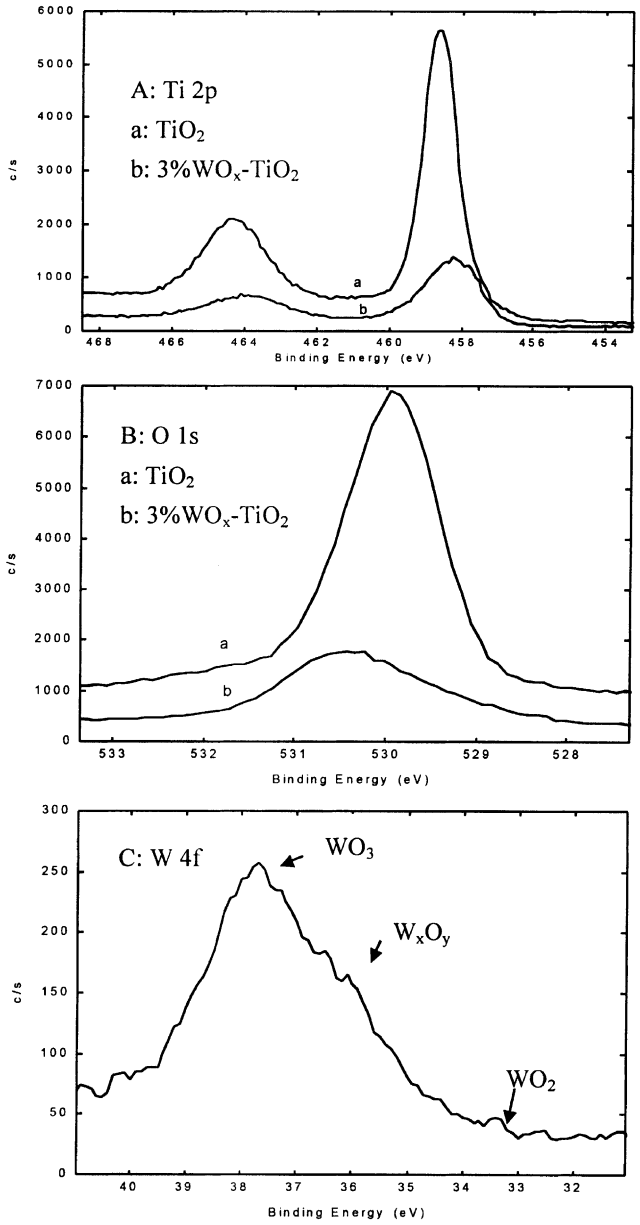

Fig. 7. The XPS fitting spectra or pure TiO_2 and 3%WO_x-TiO_2 powders. (A) Ti 2p; (B) O 1s; (C) W 4f — WO_3: W^{6+} 4f spectrum, W_xO_y: a mixed spectrum of W^{5+} and W^{6+}, and WO_2: W^{4+} 4f.

530.58 eV for the 3%WO_x-TiO_2 agree with the O 1s electron binding energy for WO_x molecule and the peak at 529.85 eV was attributable to TiO_2. The O 1s peak of 3%WO_x-TiO_2 was smaller than that of TiO_2 due to WO_x being doped on the surface of TiO_2. These results had a good agreement with those in [29–32]. The binding energy of O 1s of WO_2 and WO_3 was 530.4 and 530.6 eV, respectively. For the pure TiO_2, the O 1s peak was also narrow with slight asymmetry and had a binding energy of 529.93 eV (FWHM = 1.27 eV). The W 4f XPS spectra are shown in Fig. 7C and the W 4f peak is boarder and deformed. The fitting analysis indicated that the tungsten in the 3%WO_x-TiO_2 may present in the mixed valence of W^{4+} (2.39%), $W_xO_y{}^{n-}$ (W^{5+}) (36.91%), W^{6+} (60.70%). The results of XPS showed the existence of WO_2, WO_3, and some non-stoichiometric tungsten oxides such as $W_{12}O_{39}{}^{n-}$. Su [30] and Scholz [29] reported similar results. Vermaire and van Berge [33] proposed that the stoichiometric ion exchange between W^{4+} and Ti^{4+} might occur. In fact, W^{4+} can substitute Ti^{4+} in the lattice of TiO_2 because of the similarity in the ion radius of W^{4+} and Ti^{4+}, the bond lengths to W–O and Ti–O and the crystal structures of WO_2 and TiO_2. So, nonstiochiometric solid solution of $W_xTi_{1-x}O_2$ would form, as described therein before. Solid solution of $W_xTi_{1-x}O_2$ could lead to produce a tungsten impurity energy level, as described thereinafter.

3.5. Photoluminescence spectra and electron/hole recombination

The photoluminescence (PL) emission spectra have been widely used to investigate the efficiency of charge carrier trapping, immigration and transfer, and to understand the fate of electron/hole pairs in semiconductor particles [50]. TiO_2 powder shows a broad PL emission band. The peak position of the emission band for rutile powder is about 450 nm and that of anatase powder is about 500 nm [51]. In this study, the PL emission spectra of all samples were examined in the wavelength range of 350–700 nm as shown in Fig. 8. To illustrate the results in the figure, the positions of individual PL emission peaks are listed in Table 2. It is observed that an intensive yellowish green PL spectrum (broad band) of the pure TiO_2 is much higher than that in the spectra of WO_x-TiO_2 samples. The PL intensity greatly decreased

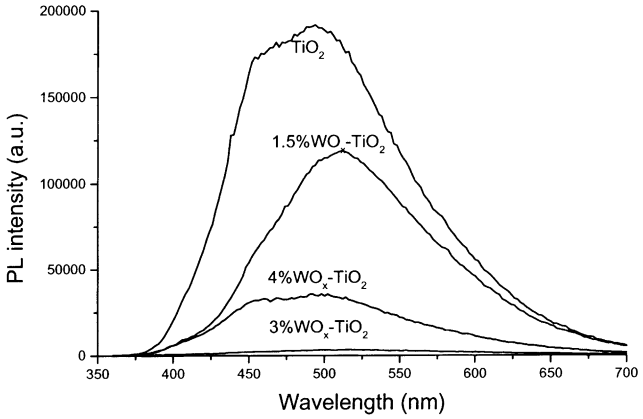

Fig. 8. The photoluminescence (PL) spectra of pure TiO_2 and WO_x-TiO_2.

due to doping tungsten oxides although the PL intensity increased back slightly when the content of tungsten oxides exceeded 3.0%. The observed PL spectra can be attributed to the radiative recombination process of either self-trapped excitons [52,53] or hydroxylated Ti^{3+} surface complexes [54] from the charge transfer excited state of the highly dispersed titanium oxide species. However, in this study there was no any fitting peak of Ti^{3+} for the 3%WO_x-TiO_2 found in the XPS analysis. The reduction of PL intensity indicates the decrease of radiative recombination process. The experimental results demonstrated that PL spectra are quite sensitive to the doping of tungsten oxide. The variation of PL intensity may result from the change of defect state on the shallow level of TiO_2 surface [55]. However, the study of defect sites on the WO_x-TiO_2 surface was not conducted in this investigation and it would be an interesting point in a further study using SEM. Similar quenching in the luminescence intensity has also been observed for In-, Ce- and Pb-doped TiO_2 by Tang et al. [52,53], Toyoda et al. [56], and Rahman et al. [57].

On the basis of the relevant band positions of WO_3 and TiO_2, photogenerated electrons are transferred from TiO_2 conduction band to the WO_3 conduction band and the holes accumulate in the TiO_2 valence band. Hence, photogenerated electrons and holes were efficiently separated. On the other hand, when the content of tungsten oxides was lower than its optimal ratio, tungsten impurity energy level would be a separation center. On the contrary, when the content of tungsten oxides was higher than its optimal ratio, tungsten impurity energy level would be a recombination center. These results also indicate that the positions of PL peaks for the modified TiO_2 catalysts apparently shifted to red direction. The shift of the emission peak toward longer wavelengths further supports the lowering of the bandgap of TiO_2 due to the tungsten oxide doping treatment.

3.6. Surface photovoltage spectra (SPS)

The relationship between the surface photovoltage of material and wavelength can provide some information about the surface state and photosensitization of the material. The photovoltage response arose from the generation of electron/hole pairs by photoexcitation. Light absorption usually leads to a direct transition from the valence band to the conduction band, with the production of electron/hole pairs. However, the generation of a photovoltage response is the direct result of free carriers. Light absorption often causes excitons rather than free carriers. The excitons must dissociate into free carriers for the production of photovoltage [39–42]. Fig. 9A shows the SPS of pure TiO_2 and 1.5%WO_x-TiO_2. To illustrate the results in this figure, the positions of peaks are listed in Table 3. The positive peaks at 336 nm for the pure TiO_2 and at 340 nm for the 1.5%WO_x-TiO_2 were attributed to the electrons excited from valence band to conduction band. The response at 436 nm for the 1.5%WO_x-TiO_2 might be attributable to the electron excited from valence band to oxygen absorbed by this catalyst. The response of the pure TiO_2 present at 389, 568 and 577 nm. The small peaks at 555, 595, 650 nm and so on for the 1.5%WO_x-TiO_2 might be attributable to the tungsten impurity energy level. Since the self-established field of samples was quite weak, the electric-field-induced surface photovoltage spectroscopy (EFISPS) was applied to produce strong photovoltage response in our investigation. Fig. 9B shows the EFISPS of TiO_2 and WO_x-TiO_2 samples. When a positive electric field (+2.0 V) was applied, photoinduced electrons diffused to the surface and holes diffused into the body [43]. The strongest peak (a) was attributed to electrons excited from valence band to conduction band, and the second strongest peak (b) was attributed to electron excited from valence band to oxygen molecule for all samples. When electron was trapped by O_2 absorbed on the surface of TiO_2, the surface state of O_2^- formed. These results agree with that reported by Cao et al. [44]. Only for the tungsten oxides-doped samples, four peaks (c, d, e, f) significantly present in the region of 500–800 nm. The positions of all peaks shift to red direction owing to the tungsten oxides in comparison with that of pure TiO_2. The SPS peaks attributable to the electrons excited from valence band to conduction band for WO_3 should not present in this region because its band gap is about 3.2 eV. So these peaks should be attributable to tungsten impurity energy level. On the other hand, the change of the intensity of EFISPS could be explained from the conversion of excitons into separate electron/hole pairs. The electrons excited from the valence band of TiO_2 would be trapped by surface oxygen and tungsten impurity or would transfer to the conduction band owing to tungsten oxides doping. The electron/hole pairs were efficiently separated. The conversion from electrons excited to free carriers would be hindered. Therefore, the intensity of EFISPS decreased with tungsten oxides doping when its content was lower than 3%. However, when the content of tungsten oxides was higher than 3%, the tungsten impurity energy level became a recombination center from a separation center. The intensity of all peaks except for that attributable to oxygen increased. It confirmed that the order of EFISPS intensity from weak to strong had a good agree-

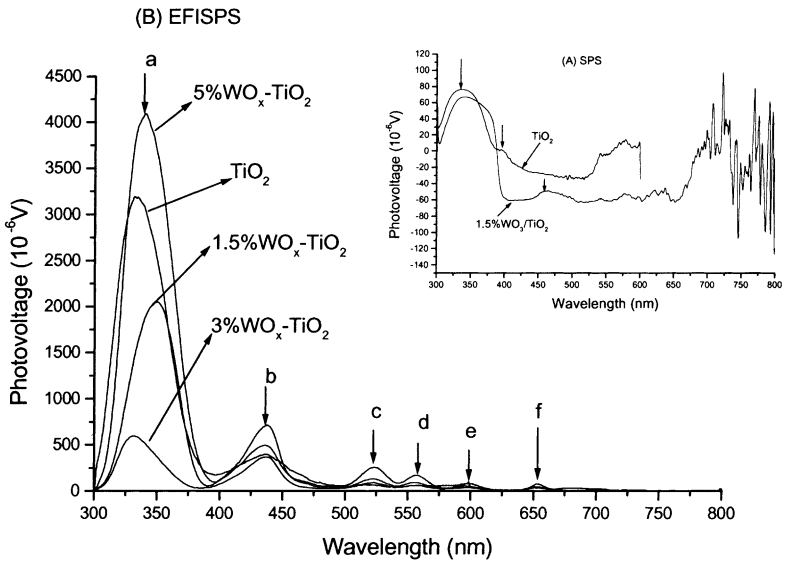

Fig. 9. The surface photovoltage spectra (SPS) (A) and electron-field-induced SPS (EFISPS) (B) when +2.0 V is applied.

ment with that of PL intensity, and with that of photoactivity from strong to weak. In this work, the reduction of EFISPS was caused by the decline of electron/hole pair recombination rate and the photoactivity is affected by electron/hole recombination greatly.

3.7. Optical absorption

According to Mie theory, TiO_2 ($E_g = 3.2$ eV) absorbs light below a threshold wavelength $\lambda_g = 387.5$ nm. However, numerous materials have given some effective ways to improve the optical absorption of TiO_2 in the visible region [34–38,45–51]. For example, the broad absorption band around 500–600 nm was ascribable to Cr-, Mn-, Ru-doping in the lattice of TiO_2 as reported by Wong and Malati [22]. The improvement of the optical absorption of Zn^+ ion implanted due to the impurity or defect level caused by the implanted Zn reported by Oyoshi et al [49]. In this study, the UV–VIS absorption spectra were measured to correspond to the optical absorption properties of photocatalysts, as shown in Fig. 10. The results indicate that all the

Table 3
The positions of the peaks of SPS and EFISPS (nm)

Samples	Peak 1	Peak 2	Peak 3	Peak 4	Peak 5	Peak 6
SPS						
TiO_2	336	389	–	568	577	–
1.5%WO_x-TiO_2	340	436	–	555	595	650
EFISPS						
TiO_2	332	435	–	–	–	–
1.5%WO_x-TiO_2	340	436	522	555	595	652
3%WO_x-TiO_2	332	437	523	557	597	653
5%Wo_x-TiO_2	340	438	524	557	600	653

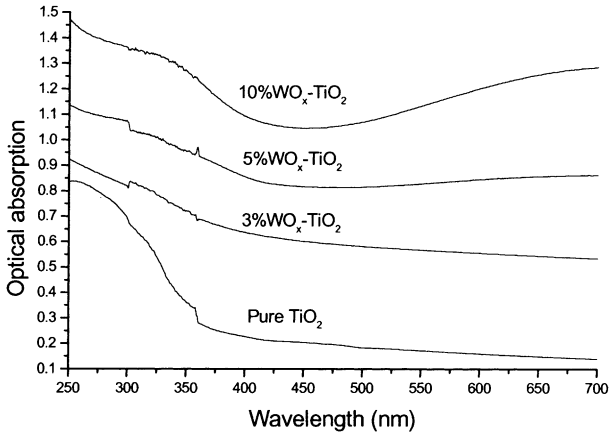

Fig. 10. The UV–VIS optical absorption spectra of pure TiO_2 and WO_x-TiO_2.

WO_x-TiO_2 samples had a better optical absorption in the region of 300–700 nm owing to the presence of tungsten oxides than the pure TiO_2. Although no clear optical absorption peak in the visible region was observed, the optical absorption edges significantly shifted to red direction. In the meantime, the results of EFISPS indicate the enhancement of photoresponse in the visible range.

To ascertain the change of light absorption band from the near UV to the visible light range found in this study, we assume that a complex of $W_xTi_{1-x}O_2$ would form in the TiO_2 doped with tungsten oxides, which had a lower energy level than that of TiO_2 as illustrated in Fig. 11. When $h\nu \geq (E_c - E_v)$, electrons can be excited in the valence band of TiO_2. When $(E_c - E_v) > h\nu \geq (E_c - E_w)$, electrons can only be excited from the $W_xTi_{1-x}O_2$ energy level. However, this assumption needs to be confirmed by defining the position of tungsten impurity ($W_xTi_{1-x}O_2$) energy level.

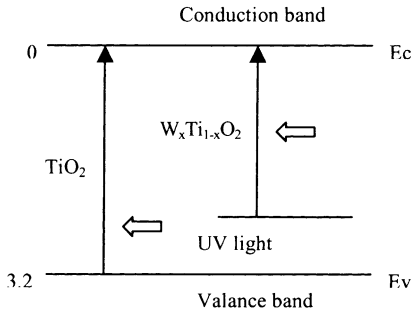

Fig. 11. The proposed tungsten impurity energy level and visible light photoinduced electron excitation.

4. Conclusions

The new photocatalyst powder of WO_x-TiO_2 was prepared by the sol–gel method and its chemical composition and optical absorption were examined by XRD, UV–VIS absorption spectra, XPS, PL, SPS, and EFISPS. The following results can be concluded:

- The photoactivity of WO_x-TiO_2 was significantly higher than that of the pure TiO_2 and an optimal content of WO_x in TiO_2 was found to be 3%.
- Tungsten oxides doping into TiO_2 could shift the light absorption band from near UV range to the visible range.
- Tungsten oxides doping into TiO_2 could hinder the recombination rate of excited electrons/holes. The order of photoactivity from weak to strong had a good agreement with that of PL intensity and that of EFISPS intensity from strong to weak.

Acknowledgements

The authors wish to thank the Hong Kong Government Research Grant Committee for a financial support to this work under the RGC Grant (RGC Number PolyU 5030/98E).

References

[1] M.R. Hoffmann, S.T. Martin, W. Choi, D.W. Bahnemann, Chem. Rev. 95 (1995) 69.
[2] D.Y. Goswami, J. Sol. ENERG-T ASME 119 (1997) 101.
[3] A. Linsebigler, G. Lu, J.T. Yates, Chem. Rev. 95 (1995) 735.
[4] F.Y. Sun, M. Wu, W.G. Li, Chin. J. Catal. 19 (1998) 229.
[5] L. Spanhel, H. Weller, A. Henglein, J. Am. Chem. Soc. 109 (1987) 6632.
[6] K.R. Gopias, M. Bohorquez, P.V. Kamat, J. Phys. Chem.-US 94 (1990) 6435.
[7] B. Idriss, P.V. Kamat, J Phys. Chem.-US 99 (1995) 9182.
[8] K. Vinodgopal, P.V. Kamat, Environ. Sci. Technol. 29 (1995) 841.
[9] J. Engweiler, J. Harf, A. Baiker, J. Catal. 159 (1996) 259.
[10] Y.R. Do, K. Lee, K. Dwight, A. Wold, J. Solid State Chem. 108 (1994) 198.
[11] G. Ramis, G. Busca, C. Cristiani, L. Lietti, P. Forzatti, F. Bregani, Langmuir 8 (1992) 1744.
[12] L.J. Alemany, L. Lietti, N. Ferlazzo, P. Forzatti, G. Busca, E. Giamello, F. Bregani, J. Catal. 155 (1995) 117.
[13] X.Z. Fu, A.C. Louis, Q. Yang, M.A. Anderson, Environ. Sci. Technol. 30 (1996) 647.
[14] W.E. Wentworth, P. Chem, J. Sol. Energy 52 (1994) 253.
[15] S.P. Fen, G.W. Meng, L.D. Zhang, Chin. Sci. Bull. 43 (1998) 1613.
[16] S.T. Martin, C.L. Morrison, M.R. Hoffmann, J. Phys. Chem.-US 98 (1994) 13695.
[17] D. Mardare, M. Tasca, M. Delibas, G.I. Rusu, Appl. Surf. Sci. 156 (2000) 200.
[18] M.M. Rahman, K.M. Krishna, T. Soga, T. Jimbo, M. Umeno, J. Phys. Chem. Solids 60 (1999) 201.
[19] K.M. Krishna, M. Mosaddeq-ur-Rahman, T. Miki, K.M. Krishna, T. Soga, K. Igarashi, S. Tanemura, M. Umeno, Appl. Surf. Sci. 113/114 (1997) 149.
[20] K. Mizushima, M. Tanaka, A. Asai, S. Iida, J. Phys. Chem. Solids 40 (1979) 1129.
[21] S.D. Mo, L.B. Lin, D.L. Lin, J. Phys Chem. Solids 55 (1994) 1309.
[22] W.K. Wong, M.A. Malati, Sol. Energy 36 (1986) 163.
[23] L. Lietti, P. Forzatti, F. Bregani, Ind. Eng. Chem. Res. 35 (1996) 3884.
[24] P. Patrono, A.L. Ginestra, G. Ramis, G. Busca, Appl. Catal. A-Gen. 107 (1994) 249.
[25] R. Weber, T. Sakurai, H. Hagenmaier, Appl. Catal. B-Environ. 20 (1999) 249.
[26] L.J. Alemany, F. Berti, G. Busca, G. Ramis, D. Robba, G.P. Toledo, M. Trombetta, Appl. Catal. B-Environ. 10 (1996) 299.
[27] F.B. Li, G.B. Gu, X.J. Li, H.F. Wan, Acta Phys.-Chim. Sinica 16 (2000) 997–1002.
[28] Z.D. Xiao, L.Y. Su, N. Gu, Thin Solid Films 333 (1998) 25.
[29] A. Scholz, B. Schnyder, A. Wokaun, J. Mol. Catal. A-Chem. 138 (1999) 249.
[30] L.Y. Su, Z. Lu, J. Phys. Chem. Solids 59 (1998) 1175.
[31] J.F. Moulder, W.F. Stickle, P.E. Sobol, K.D. Bomben, in: J. Chastain (Ed.), Handbook of X-ray Photoelectron Spectroscopy, Perkin-Elmer, Eden Prairie, MN, 1992.
[32] J.H. Scofield, J. Electr. Spectrosc. Relat. Phenom. 8 (1976) 129.
[33] D.C. Vermaire, P.C. van Berge, J. Catal. 116 (1989) 309.
[34] K. Fujihara, S. Izumi, T. Ohno, J. Photochem. Photobiol. A. 132 (2000) 99.
[35] K.M. Krishna, M. Mosaddeq-ur-Rahman, T. Miki, Appl. Surf. Sci. 113/114 (1997) 149.
[36] A. Suialu, J. Aarik, H. Mändar, Thin Solid Films 336 (1998) 295.
[37] G.H. Takaoka, T. Hamano, K. Fukushima, Nucl. Instrum. Meth. B 121 (1997) 503.
[38] M. Hiramoto, K. Hashimoto, T. Sakata, Chem. Phys. Lett. 133 (1987) 440.
[39] L. Kronik, Y. Shapira, Surf. Sci. Rep. 37 (1999) 1.
[40] Q.Z. Zhai, S.L. Qiu, F.S. Xiao, Z.T. Zhang, C.L. Shao, Y. Han, Mater. Res. Bull. 35 (2000) 59.
[41] L. Szaro, J. Rebisz, L. Misiewicz, Appl. Phys. A. 69 (1999) 409.
[42] H.H. Deng, H.F. Mao, Z.H. Lu, H.J. Xu, Thin Solid Films 315 (1998) 244.
[43] Y.A. Cao, L. Ding, Y. Ma, Z.S. Guan, T.F. Xie, X.T. Zhang, Z.Y. Wu, Y.B. Bai, T.J. Li, J.N. Yao, Y. Wu, Chem. J. Chin. Univ. 20 (1999) 1787.
[44] Y.A. Cao, T.F. Xie, X.T. Zhang, Z.S. Guan, Y. Ma, Z.Y. Wu, Y.B. Bai, T.J. Li, J.N. Yao, Acta Phys.-Chim. Sinica 15 (1999) 680.
[45] A. Kawabata, R. Kubo, J. Phys. Soc. Jpn. 21 (1966) 1765.
[46] U. Kreibig, M. Vollmer, Optical Properties of Metal Clusters, Springer, New York, 1993, p. 358.
[47] T. Sasaki, N. Koshizaki, S. Terauchi, H. Umehara, Y. Matsumoto, Nanostruct. Mater. 8 (1997) 1077.
[48] T. Yonezawa, H. Matsune, T. Kunitake, Chem. Mater. 11 (1999) 33.
[49] K. Oyoshi, N. Sumi, I. Umezu, R. Souda, A. Yamazaki, H. Haneda, T. Mitsuhashi, Nucl. Instrum. Meth. B 168 (2000) 221.

[50] H. Yamashita, Y. Ichihashi, S.G. Zhang, Y. Matrumura, Y. Souma, T. Tatsumi, M. Anpo, Appl. Surf. Sci. 121/122 (1997) 305.
[51] K. Fujihara, S. Izumi, T. Ohno, M. Matsumura, J. Photochem. Photobiol. A. 132 (2000) 99.
[52] H. Tang, H. Berger, P.E. Schmid, F. Levy, G. Burri, Solid State Commun. 87 (1993) 847.
[53] H. Tang, K. Prasad, R. Sanjines, P.E. Schmid, F. Levy, J. Appl. Phys. 75 (1994) 2042.
[54] M. Anpo, N. Alkawan, Y. Kubokaway, J. Phys. Chem.-US 89 (23) (1985) 5017.
[55] T. Toyoda, T. Hayakawa, K. Abe, T. Shigenari, Q. Shen, J. Lumin. 87–89 (2000) 1237.
[56] T. Toyoda, T. Hayakawa, Q. Shen, Mater. Sci. Eng. B78 (2000) 84.
[57] M.M. Rahman, K.M. Krishna, T. Soga, T. Jimbo, M. Umeno, J. Phys. Chem. Solids 60 (1999) 201.